Chemical enhancement in the SERS spectra of indigo: DFT calculation of the Raman spectra of indigo-Ag14 complexes

Chemical enhancement in the SERS spectra of indigo: DFT calculation of the Raman spectra of indigo-Ag_{14} complexes

Marilena Ricci[a,b], Maurizio Becucci[a,b,c,1], Emilio M. Castellucci[a,c]

[a] *Department of Chemistry 'Ugo Schiff', University of Florence, Scientific Campus, via della Lastruccia 3-13, 50019-Sesto F.no, Italy*

[b] *also at Department of Photonics, Saint Petersburg Electrotechnical University, Ul. Professora Popova 5, 197376-St. Petersburg, Russia*

[c] *also at European Laboratory for Non Linear Spectroscopy (LENS), University of Florence, Scientific Campus, via N. Carrara 1, 50019-Sesto F.no, Italy*

Keywords: Raman SERS TD-DFT Ag cluster symmetry pre-resonance NTO

1. Abstract

The appearance of the Raman and the SERS spectra of indigo (IND) at 785 and 514 nm laser wavelength excitations has prompted the study of the interactions between the molecule and the silver substrate to which the molecule is adsorbed. In particular, no change of appearance between Raman and SERS spectra, apart some intensification, is observed at 785 nm excitation whereas some changes in the number and intensity of the bands are observed at 514 nm excitation. In a previous study a simplified model has been adopted where the molecule is simply bonded to an Ag_2 cluster. Structural models have now been devised with the molecule is sited either perpendicular (*edge-on*) or planar (*surface-on*) to the surface of a Ag_{14} pyramidal cluster. The structure of the two complexes, the energy of the electronic excitations, the Raman spectra of the molecule/metal complexes have been studied through a TD-DFT simulation. The appearance of the experimental SERS spectra have been confronted with the prediction of the Herzberg-Teller surface selection rules of Lombardi et al., which have been formulated for the SERS spectra of molecules adsorbed on metal nanoparticles, in the frame of the Albrecht's theory for Raman scattering. The spectral predictions for the edge-on geometry fully meet the observation that the SERS spectra are dominated by totally symmetric A_g (under C_{2h} symmetry) bands or, taking into account the lost of the inversion center after adsorption on the metal surface, in-plane A' (under C_s symmetry) modes. This fully

[1] Corresponding author
e-mail: maurizio.becucci@unifi.it

justifies the pop up of IR modes of the molecule in the SERS spectra, modes which belong to B_u and A_u species in the free molecule C_{2h} symmetry group. A systematic assignment of the modes of the free molecule and of the molecule in the complex has been made through the inspection of the calculated vibrational coordinates of the single vibrations. Dynamic polarizability (pre-resonance) calculations have been performed at 475 and 690 nm wavelength excitations, corresponding to the experimental 514 and 785 nm wavelengths, respectively. A small spectral enhancement is predicted at 690 nm for both complex geometries which should depend on charge transfer (CT) states calculated, albeit with very weak oscillator strength, in that spectral range. A substantial enhancement is instead calculated for both the edge-on and the surface-on models at the excitation wavelength of about 475 nm. The calculated Raman spectra intensification originates from the proximity of electronic excitations of intra-cluster, intra-molecular and CT type. The plasmonic excitation can not be accounted for by the present model calculation. Natural Transition Orbitals (NTO) have been generated for the electronic excitations of both geometries, by transforming the ordinary orbital representation into a more compact form in which each excited state is expressed, if possible, as single pair of orbitals.

2. Introduction

In recent papers [1, 2, 3, 4] we have faced the study of dye molecules, alizarin, safranine and indigo, widely employed as pigments and colorants in art and manufacturing, using Raman and SERS and TD-DFT simulation of their electronic excitation energies and Raman and SERS spectra. SERS has proved a very useful spectroscopic technique for the identification of tiny amount of these molecules whose normal Raman spectra are often hindered by fluorescence emission. In general, Surface-Enhanced Raman Spectroscopy (SERS) provides a highly sensitive molecular detection method with great potential in different fields. The phenomenon of surface-enhanced Raman scattering (SERS) results in an overall enhancement of molecular Raman response by a factor up to about 10^6-10^8 due to the interaction of the molecule with rough noble metal surfaces. The signal enhancement is attributed to a strong amplification of the electromagnetic fields near the plasmon resonances of metal substrates, the so-called electromagnetic enhancement, and to atomic scale effects, which are commonly referred to as chemical enhancement.

The chemical enhancement effect is characterized by an Å-length scale and has been associated with ground state electron tunneling, formation of charge transfer or metal-molecular surface states and a substantial contribution from intramolecular resonant excitation. The determination of the absolute value of the chemical enhancement factor in surface-enhanced spectra remains a difficult problem since the measured spectra exhibit the combined effect of different mechanisms. Nonetheless, the relative chemical enhancement is found to be in reasonable agreement with the results of density functional theory modeling [1, 5]. In this contest, first principle modeling [6] revealed a useful tool that complements experimental activities and provides additional information about microscopic properties of a metal surface/adsorbed molecule interface.

Vibrational frequencies and relative Raman scattering cross sections of SERS spectra are generally different from those measured in neat samples. There exist many studies performed on the absorption and vibrational spectra, IR and Raman, of indigo and its derivatives both from the experimental and theoretical point of view [7, 8, 9, 10, 11]. We have reinvestigated [3, 12] the indigo Raman spectra with 1064, 785 and 514 nm excitation wavelengths and obtained the SERS spectra at 785 and 514 nm.

For the description of the appearance of the SERS spectra, besides the surface selection rules [13], which rely on the classical electromagnetic enhancement, other more exhaustive surface selection rules, the so-called Herzberg-Teller surface selection rules [14], have been used.

In this paper, we present time-dependent DFT simulation of SERS spectra of indigo/silver complexes. In a previous paper [3] we discussed the effects (frequency shifts and intensity enhancement of the Raman spectra) of the complexation of indigo with the Ag_2 cluster, as a function of the excitation energies. To better understand the importance of the cluster dimension and geometry, we modeled, according to previously reported examples (see [15]), different metal-molecule complexes. In particular, we extended the analysis to the larger Ag_{14} cluster in the shape of a pyramid such that not to limit the interaction to a single atomic layer. Moreover, it is now possible to set up interaction geometries between the molecule and the metal cluster such that either the molecule stands perpendicular or lays flat on the surface. The two structures correspond to edge-on and

surface-on complexes, respectively. The pyramidal shape given to the Ag_{14} cluster best simulates the bulk structure of the Ag nanoparticle at a reasonable computational cost.

These complexes should give more confidence to the outcome of the simulation of the SERS spectra. Accordingly, the chemical contribution to the spectral enhancement effect was computed, for the different model geometries. The calculated Raman spectra of the two complexes, in the static and pre-resonance condition, are confronted with the measured SERS spectra.

We studied the effects that contribute to the ground state Raman enhancement, such as the *molecular orientational effect*, the *change of local symmetry effect* and the effect of the *proximity* of one side of the molecule to a binding site of the metal cluster. With this respect the calculation of the spectra of the molecule adsorbed on metal cluster using DFT methods is a mean for the interpretation of the interaction mechanisms between the adsorbed indigo molecule and the silver nanoparticle surface. The two different interaction geometries were adopted as they can be used to elucidate the adsorption geometries in real samples.

3. Computational details

Ground-state geometry optimization, UV-VIS excitation spectra, and static and pre-resonance Raman spectra in the infinite lifetime approximation were calculated for the indigo and indigo-Ag_{14} complexes using the suite of programs Gaussian 09 [16].

Two different starting geometries were adopted: the *surface-on* model where the indigo molecule lays flat on the surface (pyramidal base) of the cluster and the *edge-on* model where the molecule stands perpendicular to it. The indigo-Ag_{14} complexes are left to adjust their geometry to a minimum of the energy surface with the Ag_{14} cluster being completely frozen in its previously optimized geometry. This caused some low frequencies due to vibrations of the whole molecule with respect to the metal cluster to be negative. Nevertheless, the final geometry can still be accepted as a structural minimum of the potential surface as only two out of the six external modes have negligible negative frequencies.

The basis set for the atoms except Ag was the 6-31g*. For silver atoms, the valence electrons and internal shells were described employing the ECP basis LANL2DZ.

The B3LYP hybrid functional provided a good accuracy in the calculation of frequency-dependent polarizabilities and Raman scattering activity.

For the optimized complex structures, the 30 lowest electronic excitations were computed using the TD-DFT method. The resulting line spectra were broadened using an empirical Lorentzian broadening parameter of 0.1 eV. The absorption maximum for the $\pi \longrightarrow \pi^*$ electronic transition of indigo has been calculated at about 550 nm (see also Ref. [3]) whereas an experimental value of 609 nm [17] is reported. The wavelengths for excitation of the Raman spectra were chosen according to the instruction reported in the Gaussian 09 User's Reference manual for pre-resonance Raman calculation and resulted, for the experimental wavelength of 785 nm, to be about 690 nm and for the 514 nm wavelength, to be about 475 nm.

As shown by Placzek polarizability theory [18] Raman intensities should be calculated with frequency dependent polarizability derivatives. For polyatomics the important quantities are the derivatives of the polarizability tensor components with respect to normal coordinates. The TD-DFT Raman intensity calculation performs numerical derivatives of the dynamic, i.e., frequency dependent, polarizability tensor elements with respect to small displacements of the cartesian coordinates along the normal modes.

In fact, the Raman activity S (Å^4/amu units), which is defined as:

$$S_k = (45{\alpha'_k}^2 + 7{\gamma'_k}^2) \tag{1}$$

is calculated for each mode k.

Here α' and γ' are the derivatives of the polarizability invariants, i.e., the mean polarizability and the anisotropic polarizability, respectively.

With observation perpendicular to the linearly polarized incoming laser beam the expression for Differential Raman Scattering Cross-Section (DRSCS), with units 10^{-30}cm^2/sr, is:

$$I^k_{Raman} = (2\pi)^4(\tilde{\nu}_{in} - \tilde{\nu}_k)^4 \frac{h}{8\pi^2 c\tilde{\nu}_k} \frac{S_k}{45} \frac{1}{[1 - exp(-hc\tilde{\nu}_k/k_B T)]} \tag{2}$$

In the equation, besides the well known universal constants, $\tilde{\nu}_{in}$ and $\tilde{\nu}_k$ are the frequencies, in cm^{-1}, of the incident light and of the kth vibrational mode. S$_k$ is the Raman

activity, which is directly obtained by the DFT calculation.

The above formula is valid within the double harmonic approximation which assumes harmonic vibrational wavefunctions and uses only the first derivatives of the polarizability with respect to nuclear displacement.

A guess of the intensification of the calculated static Raman spectra due to complexation with silver Ag_{14} clusters can be obtained as the *integrated* Enhancement Factor:

$$EF_{static}^{integr} = \frac{\sum_j S_j^{complex}}{\sum_j S_j^{indigo}} \tag{3}$$

In the case of pre-resonance calculation the EF^{integr} has been set as

$$EF_{pre-res}^{integr} = \frac{\sum_j S_j^{complex/pre-res}}{\sum_j S_j^{complex/static}} \tag{4}$$

The numerator and denominator are sum of Raman scattering activity terms over the j modes (see Tab. S1 and S2 of Supplementary Information package).

The static polarizability Raman spectra of the indigo/cluster complexes were computed to investigate the effects (frequency shifts and EFs) of the ground-state interaction between the molecule and the silver cluster. The frequency dependent DFT Raman calculations (dynamical polarizability) were carried out in the infinite life-time approximation. It is well known that in this case the Raman activity calculation for excitation at resonance gives rise to undetermined spectral intensities and a pre-resonance calculation should be instead carried-out. In this case the feasibility of the calculation is controlled by the distance from the nearest resonance and its transition strength. The weaker the transition, the closer the calculation can be carried out. The dynamic polarizability Raman pre-excitation spectra of the indigo/cluster complexes were then computed for excitation of 475 nm, for the comparison with the experimental 514 nm excitation, and of 690 nm, for the comparison with the 785 nm excitation.

The static and the frequency-dependent Raman spectra were all calculated at the same level of theory. The Raman spectra were simulated by a Lorentzian broadening of the line spectra using an empirical linewidth of 5 cm^{-1}. The computed frequencies are reported by application of a scaling factor of 0.960.

4. Results and Discussion

4.1. Experimental Raman and SERS spectra

The experimental details are reported in previous papers [3, 12]. The spectra shown were corrected for the instrumental response.

Although the expected reduced molecular symmetry in the complex should give rise to a SERS spectrum differing from the corresponding Raman spectrum of the C_{2h} free molecule, the reduction of symmetry is not appreciated however in the SERS spectra taken far from resonance, i.e., at 785 nm, as no noticeable spectral changes are observed. The Raman and SERS spectra look very similar (see Fig. 1).

Some changes in relative intensity and the occurrence of new Raman bands are instead observed in the SERS spectrum at 514 nm excitation, due to the closeness to the molecular electronic transition (about 609 nm) and the plasma absorption (about 420 nm) of the nanoparticle silver colloid used as SERS substrate. The new bands arise through the reduction of symmetry (the center of symmetry is lost) of the molecule after complexation, from C_{2h} to C_s (see Fig. 2) and can be assigned as A_u and B_u, i.e., IR active only, bands under the C_{2h} molecular symmetry or as A' (in-plane) and A" (out-of-plane) modes in the new, reduced symmetry in the complex (see Tab. S1 and S2 of the Supplementary Information package).

4.2. The surface selection rules

Surface selection rules for SERS were conceived [13] in the frame of the electromagnetic enhancement mechanism. If this is the active mechanism, the Raman modes with polarizability component of the type $\alpha_{\rho\rho}$ with $\rho = x, y, z$, are, in turn, maximally enhanced in SERS provided the axis of the polarizability tensor of the molecule is oriented perpendicularly to the metal surface and parallel to the plasmon field. Assuming z to be the axis, the component α_{zz} will be preferentially enhanced. Minor enhancement should also be observed for the α_{xz} and α_{yz} components. However other enhancement mechanisms can be present, which are grouped in the so called "chemical enhancement". These are the: ground state, molecular resonance and charge transfer mechanisms, respectively. The first and third mechanism need a chemical interaction (first layer effect) of the molecule with the metal surface. The enhancement due to the molecular electronic resonance can occur

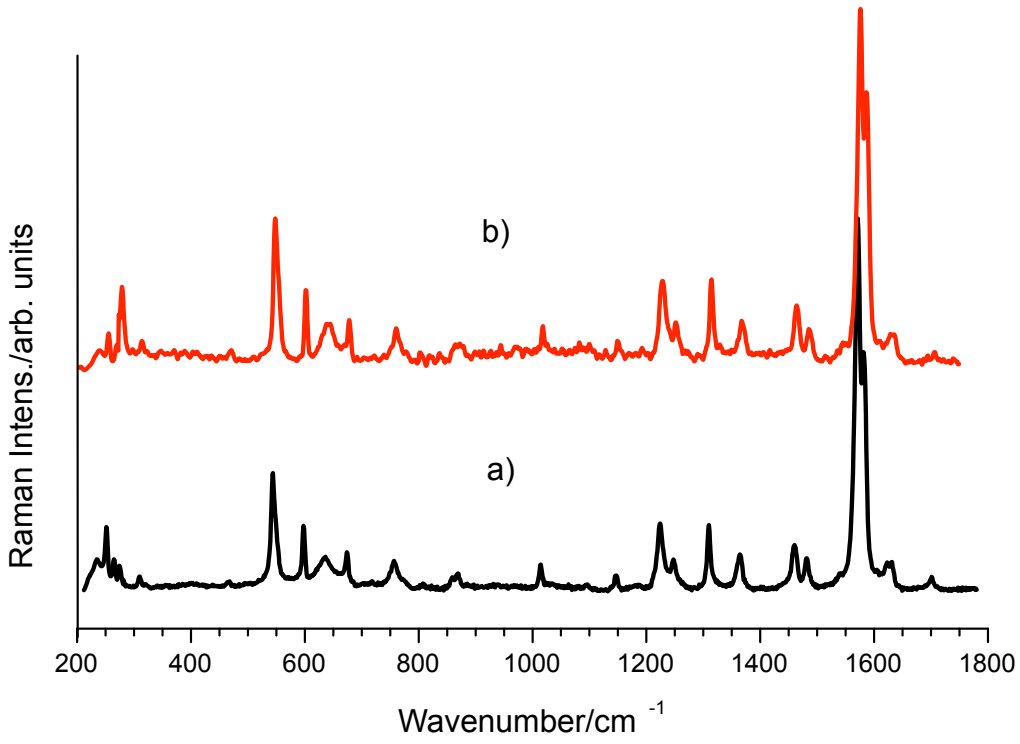

Figure 1: Experimental: a) Raman and b) SERS, spectra of indigo at 785 nm excitation wavelength; spectra are baseline subtracted and normalized

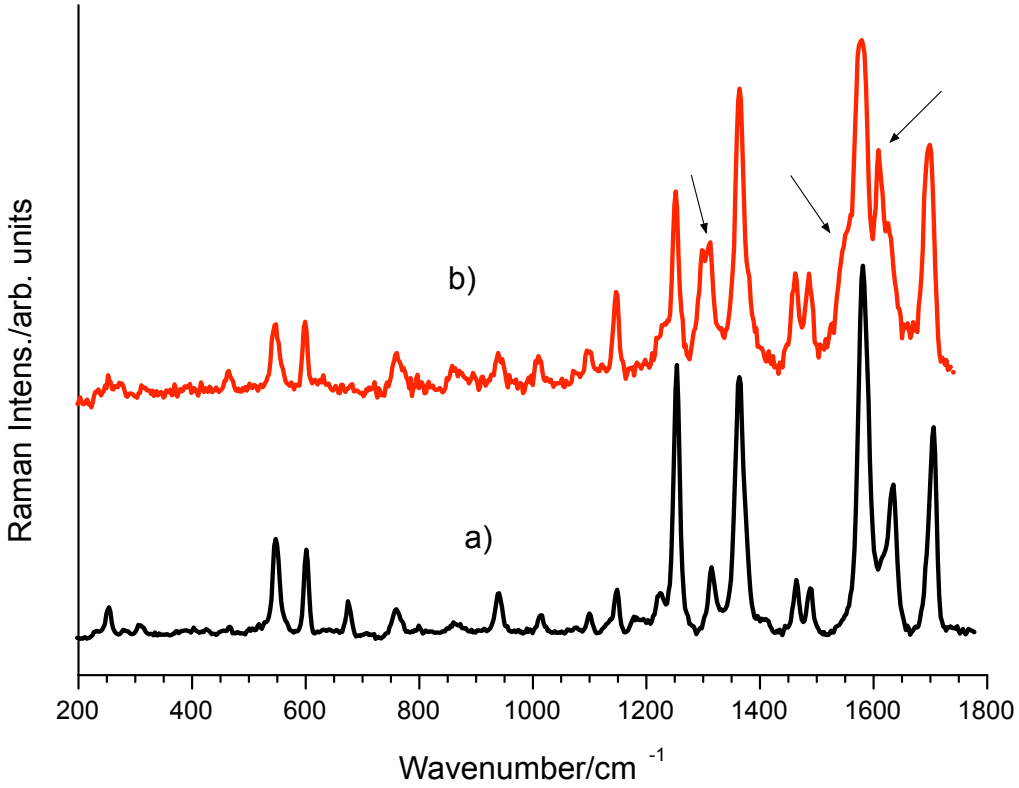

Figure 2: Experimental: a) Raman and b) SERS, spectra of indigo at 514 nm excitation; spectra are baseline subtracted and normalized; $\longleftarrow$ indicate new Raman activated bands

anyway provided the laser excitation matches an electronic resonance of the molecule, both free or bound to the metal.

In principle, the different enhancements can be selected using different excitation wavelengths, provided the plasmon, electronic and charge transfer resonances occur at different energies. Their contribution to the enhancement can be factors of ten whereas the ground state interaction will contribute few units only. If the resonances are almost coincident the SERS enhancement can be very high.

A more general approach to SERS is due to Lombardi and Birke [19] which adapted the Albrecht [20], Herzberg-Teller scattering model, to the metal-molecule complex by adding to the electronic states the metal-molecule charge-transfer (CT) states which borrow their intensity from the allowed molecular electronic transitions. A general formula for polarizability was adopted which considers the presence of the three resonances, i.e., plasmon, molecular and charge-transfer, the intramolecular electronic and charge-transfer transition dipole moments, the harmonic oscillator vibrational integral and the Herzberg-Teller coupling term.

In presence of one or more of the three resonances, the SERS surface selection rules can be achieved through the numerator of the formula. The Moskovits's surface selection rules, are also considered in the H-T surface selection rules.

In the case of indigo SERS spectra is important to define the range of electronic excitations. For excitation at 785 nm, the plasmonic resonance, measured at about 420 nm, and the molecular resonance, at about 609 nm, can be considered ineffective with respect to the enhancement. Only CT resonances, if present in this range, can contribute, directly through the A term and/or through the B (molecule-to-metal charge-transfer) or C (metal-to-molecule charge-transfer) term of the Albrecht's type Raman scattering formulation. The Raman and SERS spectra should be anyway different due to the degradation of symmetry of the molecule by complexation with the metal cluster which brings about the activation in the SERS of the IR, "ungerade" modes, not allowed in the Raman spectrum of the indigo molecule which exhibits a C_{2h} point group symmetry. This is however not verified in this experiment (see Fig. 1) where the Raman and SERS spectra look very similar.

Different things occur for excitation at 514 nm. In this case, both the plasmon and the molecular resonances are closer and a higher enhancement is expected. The two resonances should be the major contributors to the enhancement. The Raman spectrum becomes a pre-Resonance Raman (RR) spectrum (see Ref. [3]) and the SERS spectrum should be further enhanced by the plasmonic and, possibly, by the charge-transfer resonances. Besides more bands are also expected in this case (see discussion above) due the reduction of symmetry which occurs to the indigo molecule. The center of symmetry of the molecule is lifted by the complexation which would bring the molecular symmetry from C_{2h} to C_s and the symmetry species will correlate as follow: A_g and B_u to A' (in-plane modes) and B_g and A_u to A" (out-of-plane modes). The Raman and the SERS spectra look now different, at least in the higher frequency range, between 1200 and 1800 cm^{-1}. New bands appear: 1611 (s), 1507 (sh), 1326 (m), which originally belonged to the "ungerade" species in the molecule. The lower frequency range, below 1200 cm^{-1}, does not exhibit noticeable changes (see below, however).

We can now apply the selection rules derived from the Eq. 15 of Ref. [14]. Preliminary to the discussion on the selection rules is the assumption of the structural geometry of the metal-molecule complex. Let us assume a edge-on, perpendicular, geometry (see Fig. 3).

According to the numerator of the expression for polarizability (Eq. 15 of Ref. [14]), in presence of the three type of resonances, i.e., plasmonic, charge transfer and molecular, it is possible to infer the selection rules which govern the appearance of vibrational bands in the SERS spectra of metal complexes. Four parameters govern the so-called Herzberg-Teller (H-T) surface selection rules: $\mu_{KI}\mu_{FK}h_{IF} < i|Q_k|f >$, where $|K >$ and $|I >$ where $|K >$ and $|I >$ are molecular states and $|F >$ cluster states at the Fermi energy. The first two terms are electronic transition moments, then we have the H-T coupling term and a term for harmonic oscillator transition of the vibrational mode k of the SERS spectrum. The expression deals with CT transitions between the Fermi state of the metal $|F >$ and the molecular state $|K >$ which draw intensity, through the H-T coupling term h_{IF} which couples the ground molecular state $|I >$ and the Fermi level state $|F >$, from the allowed electronic transition $|I > \rightarrow |K >$. The scheme corresponds to the C Albrecht's type term

of the polarizability for the metal/molecule complex (see Ref. [14]).

In fact, the H-T selection rule expression consists of the direct products of the dipole operators' symmetry species and the symmetry species of the H-T coupling operator $(\partial/\partial Q_k)$, which behaves as a vibrational coordinate, and of the harmonic oscillator transition term for mode k. The vibrational integral is different from zero only for a harmonic oscillator transition between the initial and the final vibrational level of the mode k, i.e., $f = i \pm 1$. The symmetry of the CT transition dipole depends on the adsorption geometry of the molecule on the nano-particle surface. With the assumed edge-on geometry the CT transition dipole moment will be aligned with the plasmonic electric field which develops mainly perpendicularly to the nano-particle surface. The interaction will be maximum in this case. For the indigo C_{2h} molecule adsorbed according to edge-on geometry the CT transition dipole direction will be in the molecular xy plane and will behave as a B_u species. The H-T surface selection rules for harmonic oscillator type SERS bands can then be cast (see Ref. [14]) as:

$$\Gamma(Q_k) = \sum (\mu_{CT}^{\perp}) \times \Gamma_K \tag{5}$$

The symmetry species of the more enhanced bands in the SERS spectrum will depend on the direct product of the species of the CT transition (B_u) and that of the molecular upper state (B_u or A_u), provided the electronic transition oscillator strength is large enough. In the case of the indigo molecule, a planar, centro-symmetric, molecule belonging to the C_{2h} point group, the species of the SERS bands will be then either $B_u \times B_u = A_g$ or $B_u \times A_u = B_g$, according to the symmetry species of the electronic states of the molecule. In the case of the degradation of the molecular symmetry from C_{2h} to C_s in the complex, the correlation between the species of the two groups brings to a A' (in-plane) symmetry for the H-T transition moment and A' (in-plane) or A" (out-of-plane) species for the electronic allowed transition.

The only electronic absorption bands which exhibit reasonable oscillator strength are of B_u (A', in-plane) type (see Tab. 1). This claims the A_g (A', in-plane) species bands to be the only bands with appreciable intensity in the SERS spectra.

Besides, also the new bands observed in the SERS spectrum at 514 nm originate from

in-plane B_u species of the free molecule (see Ref. [12] for assignment) and are classified as in-plane A' modes.

In the frequency region below 1000 cm^{-1} of the SERS spectrum at 514 nm excitation, where also out-of-plane A" bands (B_g and A_u in the free molecule symmetry) are expected, only A_g (A', in-plane) species bands have reasonable intensity, as shown in Fig. 2. The only exception is the band at 582 cm^{-1}, assigned in the Raman spectrum as a B_g species at 602 cm^{-1}, which correlates to a A" (out-of-plane) species mode in the SERS. No relative enhancement is observed for this band however, by comparing the Raman and SERS spectra. Other modes, i.e., 860, 761 and 465 cm^{-1}, assigned in the Raman spectrum to B_g species and A" out-of-plane species in the SERS spectrum, exhibit a dubious, however tiny, enhancement. Not well defined is the behavior of the group of weak/very weak bands around 250 cm^{-1} in both spectra. We conclude that only the A_g and B_u modes of the Raman spectrum (A' in-plane modes in the SERS spectrum) exhibit an appreciable enhancement (see, for instance, the bands at 1486, 1468, 1310, 1252 and 1147 cm^{-1} of the SERS spectrum). This is in line with the prediction of the H-T selection rules.

Assuming the molecule to be adsorbed on the surface in a surface-on geometry, the CT transition dipole moment should behave as an out-of-plane species, i.e., A_u (A" in the reduced symmetry group C_s). In this case the H-T surface selection rules would predict the species more enhanced in the SERS spectra to be $B_u \times A_u = B_g$ or $A" \times A' = A"$. The dubious enhancement observed for few bands (see above) of out-of-plane A" symmetry does not allow the choice of such a structure.

Table 1: Calculated excitation energies of the indigo C_{2h} molecule

nm	eV	Oscillator strength	Symm	MO transition
548.21	2.26	0.2724	B_u	68 → 69
325.92	3.80	0.2346	B_u	65 → 69
304.28	4.07	0.0598	B_u	62 → 69
281.32	4.41	0.2061	B_u	68 → 71
271.45	4.51	0.5546	B_u	67 → 70

4.3. Geometry optimization

The optimized geometries of the complexes are shown in Fig. 3.

The relevant structural parameters of the indigo-Ag_{14} complexes, i.e., Ag-O distance, Ag-N distance, angle between the base of the pyramidal Ag_{14} cluster and the molecular

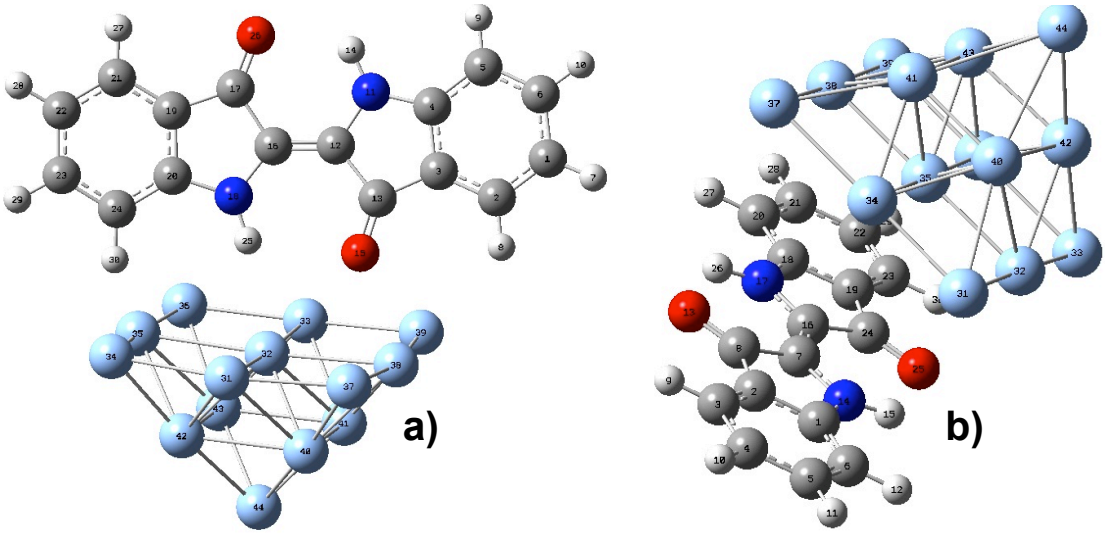

Figure 3: Optimized structures of IND-Ag_{14} complexes: a) edge-on, b) surface-on

plane, are reported in Table 2:

Table 2: Geometric parameters of the indigo-Ag_{14} complexes

Complex	Ag-OC distance[a] (Å)	Ag-NH distance[a] (Å)	angle[b] (degrees)
surface-on	5.33106(13-35)	4.65938 (14-35)	3
	4.61086(25-35)	4.61784(17-35)	
edge-on	3.29338(15-32)	3.57678(18-32)	87

[a] numbers in parentheses are atom labels (see Fig. 3)
[b] angle between the molecular plane and the base of the pyramidal cluster

4.4. Electronic excitation spectra

The calculated energy excitation spectra of the indigo-Ag_{14} complexes are shown in Fig. 4. The vertical arrow lines indicate the excitation wavelengths of 475 and 690 nm used for the calculated pre-resonance Raman spectra.

In the case of the indigo-Ag_{14} complexes the excited states resulted very often a mixed composition of orbital transitions without any dominant component which should be simplified by the Natural Transition Orbital (NTO) method developed by Martin [21]. These are reported, for transitions in the range 400 - 700 nm, in Tab. 3. Few examples are shown in Fig.s S1 and S2 of the Supplementary Information package. The NTO transition occurs from excited *particle* (occupied) to the empty *hole* (unoccupied). These are tagged in Tab. 3 as H, for occupied and L, for unoccupied.

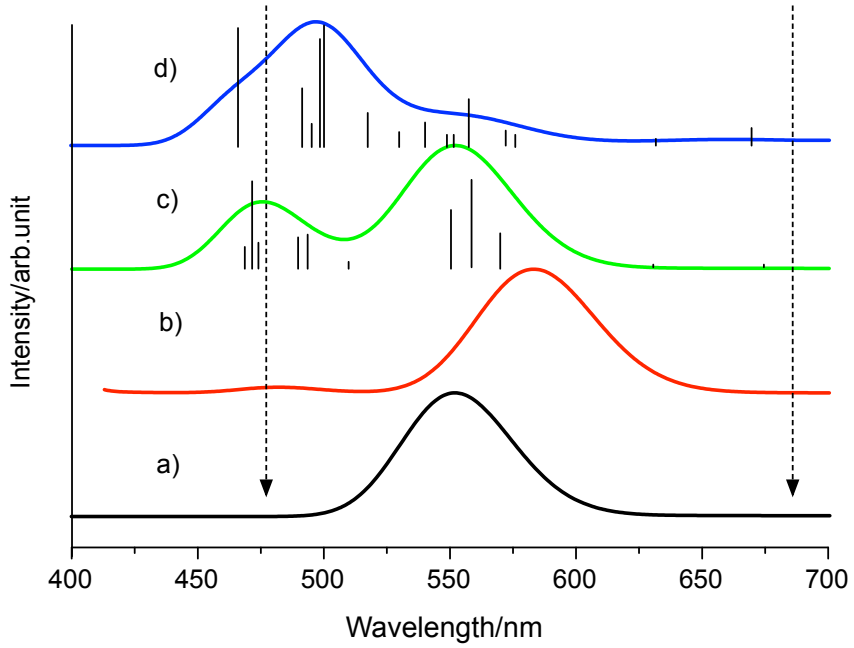

Figure 4: Calculated electronic excitations of: d) indigo-Ag_{14} surface-on and c) indigo-Ag_{14} edge-on complex; vertical bars indicate the single excitations to which a Lorentzian width of 0.1 eV is applied; the dotted line arrows indicate the excitation wavelengths (about 475 and 690 nm) of the pre-resonance Raman spectra calculation; the calculated electronic spectra of: b) indigo-Ag_2 complex and a) indigo, are also reported

Table 3: Electronic excitations of the indigo-Ag_{14} complexes calculated in the range 400 - 700 nm. The NTO orbital transitions with coefficients and the orbital character of each are also reported.

Complex	#	**Wavelength (nm)**	**Oscillator strength**	**NTO**[a] **transition**	**Coefficient**	**Character**[b]
edge-on	12	697.77	0.0001	H → L	0.95301	intracluster
	13	677.59	0.0005	H → L	0.98684	CT
	14	662.01	0.0011	H → L	0.99251	CT
	15	640.78	0.0002	H → L	0.68410	intracluster
				H-1 → L+1	0.23108	intracluster
	16	630.60	0.0009	H → L	0.69947	intracluster
				H-1 → L+1	0.22777	intracluster
	17	569.12	0.0171	H → L	0.50381	intracluster
				H -1→ L+1	0.37496	CT
	18	558.63	0.0975	H → L	0.60998	intracluster
				H-1 → L+1	0.21954	mixed
	19	551.50	0.0497	H → L	0.79706	CT
				H-1 → L+1	0.15679	intracluster
	20	547.81	0.1618	H → L	0.72663	$\pi \rightarrow \pi^*$
				H-1 → L+1	0.12646	intracluster
	21	522.83	0.0018	H → L	0.98594	intracluster
	22	510.15	0.0064	H → L	0.98835	CT
	23	492.95	0.0263	H → L	0.64090	intracluster
				H-1 → L+1	0.28237	intracluster
	24	489.76	0.0167	H → L	0.66135	intracluster
				H-1 → L+1	0.26583	intracluster
	25	478.06	0.0023	H → L	0.85063	CT
				H-1 → L+1	0.13403	intracluster
	26	473.59	0.0138	H → L	0.40992	intracluster
				H-1 → L+1	0.26047	CT
				H-2 → L+2	0.22740	intracluster
	27	472.95	0.0090	H → L	0.42447	intracluster
				H-1 → L+1	0.37002	intracluster
				H-2 → L+2	0.18403	CT
	28	472.83	0.1142	H → L	0.89076	intracluster
	29	468.91	0.0082	H → L	0.90916	CT
	30	456.88	0.0004	H → L	0.98897	intracluster
surface-on	13	668.40	0.0103	H → L	0.77613	mixed
				H-1 → L+1	0.13342	intracluster
	14	642.11	0.0010	H → L	0.93659	CT
	15	632.97	0.0036	H → L	0.91597	CT
	16	610.69	0.0003	H → L	0.85555	intracluster (mixed)
	17	577.75	0.0049	H → L	0.77494	intracluster
				H-1 → L+1	0.21134	$\pi \rightarrow \pi^*$ (mixed)
	18	573.06	0.0097	H → L	0.71704	CT
				H-1 → L+1	0.16118	intracluster
				H-2 → L+2	0.11923	intracluster
	19	555.32	0.0373	H → L	0.82836	$\pi \rightarrow \pi^*$ (mixed)
				H-1 → L+1	0.15039	mixed
	20	551.49	0.0037	H → L	0.59124	$\pi \rightarrow \pi^*$
				H-1 → L+1	0.23103	CT
	21	549.07	0.0038	H → L	0.77396	intracluster
				H-1 → L+1	0.10082	$\pi \rightarrow \pi^*$ (mixed)
	22	539.21	0.0079	H → L	0.90088	CT
	23	532.13	0.0040	H → L	0.98844	CT
	24	517.62	0.0191	H → L	0.95324	CT
	25	499.72	0.1013	H → L	0.52277	intracluster
				H-1 → L+1	0.21008	mixed
	26	498.90	0.0950	H → L	0.58688	intracluster
				H-1 → L+1	0.25659	intracluster
				H-2 → L+2	0.11957	intracluster
	27	495.97	0.0110	H → L	0.92793	intracluster
	28	491.72	0.0415	H → L	0.75174	mixed
				H-1 → L+1	0.13163	intracluster
	29	466.16	0.1014	H → L	0.91811	intracluster
	30	461.15	0.0008	H → L	0.77030	intracluster
				H-1 → L+1	0.10894	intracluster

[a] see Ref. [21]; H=*particle* (occupied), L=*hole* (unoccupied)
[b] CT = charge-transfer; mixed character: CT, intramolecular, intracluster

4.5. Calculated static Raman spectra

The calculated static Raman spectra of the complexes are shown in Fig. 5. The comparison is made with the experimental FT-Raman spectrum at 1064 nm which is supposedly similar to the corresponding SERS spectrum.

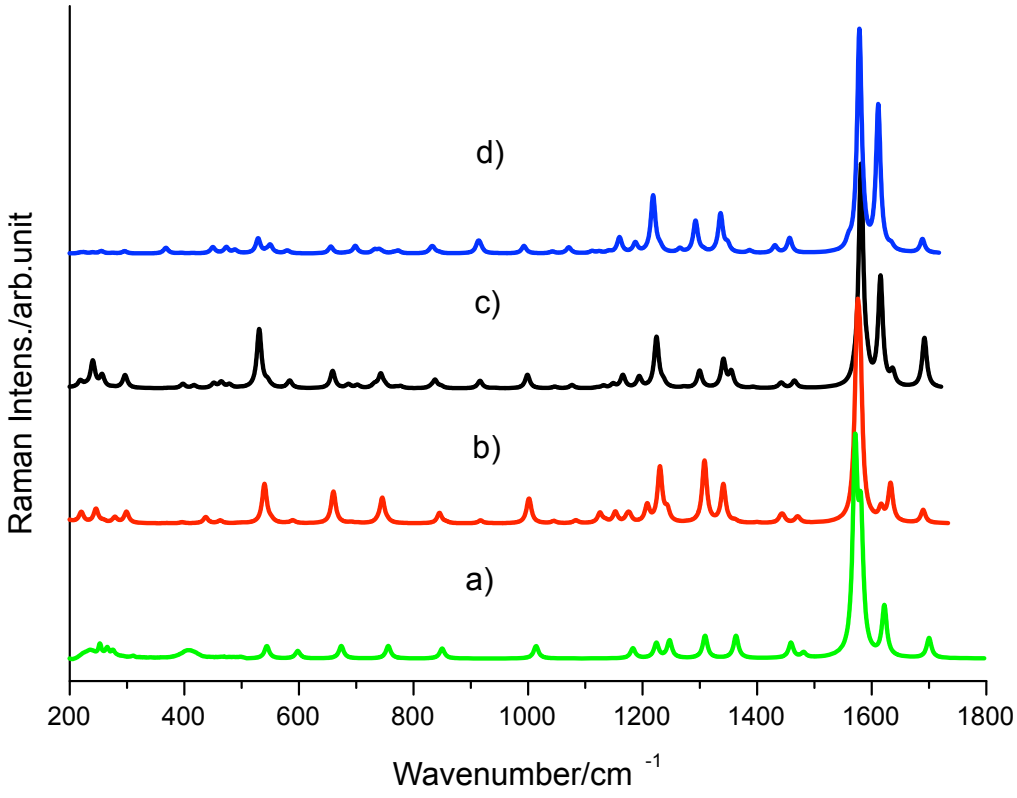

Figure 5: Calculated static Raman spectra of indigo-Ag_{14} complexes with different geometries: d) surface-on and c) edge-on; the calculated Raman spectra of: b) the indigo-Ag_2 complex and a) the experimental Raman spectrum of indigo at 1064 nm excitation, are also reported; a scaling factor of 0.960 is applied; intensity correction (see Eq. 2) applied

The bands of the calculated static Raman spectra of the edge-on and surface-on complexes, in the region up to 1800 cm^{-1}, are reported in Tab. S1 and S2 of the Supplementary Information package, respectively.

The assignment of the bands follows the PED description, i.e., the bands in the different spectra with analogous PED description as the indigo molecule are assigned to the same vibrational modes. Each mode is given its symmetry species, both under the point group C_{2h} for the free molecule and of the point group C_s for the molecule in the complex.

The frequency shifts with respect to the calculated static spectrum of indigo are also

reported for the two complexes, in Tab. S1 and S2 of the Supplementary Information package, respectively.

The calculated IR active (A_u and B_u species) bands of the indigo spectrum exhibit zero Raman activity according to the C_{2h} symmetry of the molecule. The mutual exclusion rule is no longer valid in the spectra of the complexes where the centro-symmetry is lifted. The corresponding bands in the SERS spectra (in-plane, A' and out-of-plane, A") acquire then some intensity, as discussed above. The stronger bands in the edge-on geometry complex correspond to modes largely of $\nu_{C=C}$ and $\nu_{C=O}$ type. This is also the case for the corresponding bands in the surface-on.

The integrated EF^{integr}_{static} for the calculated static Raman bands of the edge-on and surface-on complexes, are reported in Tab. 4. Practically, no enhancement occurs in both complexes. The corresponding EF for the IND-Ag_2 complex is similar, as reported in Ref. [3].

A very small positive shift for the bands in the more significant region up to 1800 cm^{-1} is obtained for both the complexes. It is worth noting however, that the modes (in both complexes) which exhibits the higher, negative, shift have $\nu_{C=O}$ and δ_{NH} component vibrations. Negative shifts are also calculated for other modes which contains the $\nu_{C=C}$ vibration. The higher, negative, shifts are however exhibited by the edge-on complex.

The $C = O$, $N - H$ and $N - C = C - N$ groups seem then to interact with the surface Ag atoms of the cluster more than other groups (benzene rings, $C - H$ groups). The interactions seem to be stronger in the case of the edge-on complex due to the higher, negative, shifts and to the proximity of the groups to the surface as shown by the geometrical parameters, i.e., atom distances and angles, reported in Tab. 2.

4.6. Calculated pre-resonance Raman spectra

In Fig. 6 the calculated pre-resonance Raman spectra of the two complexes at about 690 nm are confronted with the experimental SERS spectrum at 785 nm.

The spectral similarity of the experimental and the calculated spectra is fairly good. The $EF^{integr}_{pre-res}$ for the Raman bands of the edge-on and surface-on complexes are reported in Tab. 4. In the case of the Ag_2 complex the EF (see Tab. 2 of Ref. [3]) at 690 nm, resulted a little bit higher.

Table 4: The EF^{integr}_{static} and $EF^{integr}_{pre-res}$ calculated for the edge-on and the surface-on indigo-Ag_{14} complexes

	$EF^{integr\,a)}_{static}$	$EF^{integr\,b)}_{690}$	$EF^{integr\,b)}_{475}$
edge-on	0.8	13.4	362.6
surface-on	0.6	14.5	204.5

[a)] see Eq. 3; [b)] see Eq. 4

The low enhancement calculated for both the edge-on and the surface-on complex for excitation at about 690 nm (experimental wavelength 785 nm) is definitely of chemical type and should be due to CT excitations of very small oscillator strength calculated in that range (see Fig. 4 and Tab. 3.). In the H-T coupling model the terms of polarizability which give the contribution to the intensity should be in this case the Albrecht's type C and A terms which, both, contribute to the intensity of totally symmetric species (see Ref. [14]).

As far as the Raman spectra of the two complexes, calculated in pre-resonance condition at about 475 nm, they are reported in Fig. 7 where they are confronted with the experimental SERS spectrum at 514 nm. The numerical data and assignment are reported in Tab. S1 and S2 of the Supplementary Information package. In this case the spectra exhibit a quite noticeable intensification due to the proximity of the excitation to electronic excitations (see Fig. 4). The calculated $EF^{integr}_{pre-res}$ are 362.6 and 204.5 (see Tab. 4), for the edge-on and the surface-on complex, respectively. These values are of the same order of magnitude as the calculated EF^{integr} in the case of the Ag_2 complex[3]. The appearance of the spectra compares only fairly with the experimental spectrum at 514 nm. Nevertheless, the main spectroscopic features are reproduced in the spectra. The closeness of the $EF^{integr}_{pre-res}$ at 475 nm excitation with the EF value at the same wavelength for the indigo-Ag_2 complex (see Ref. [3]) is not surprising as the type of interaction geometry between the molecule and the metallic surface, i.e., the $C = O$ and $N - H$ groups pointing to the Ag atoms of the surface, is analogous.

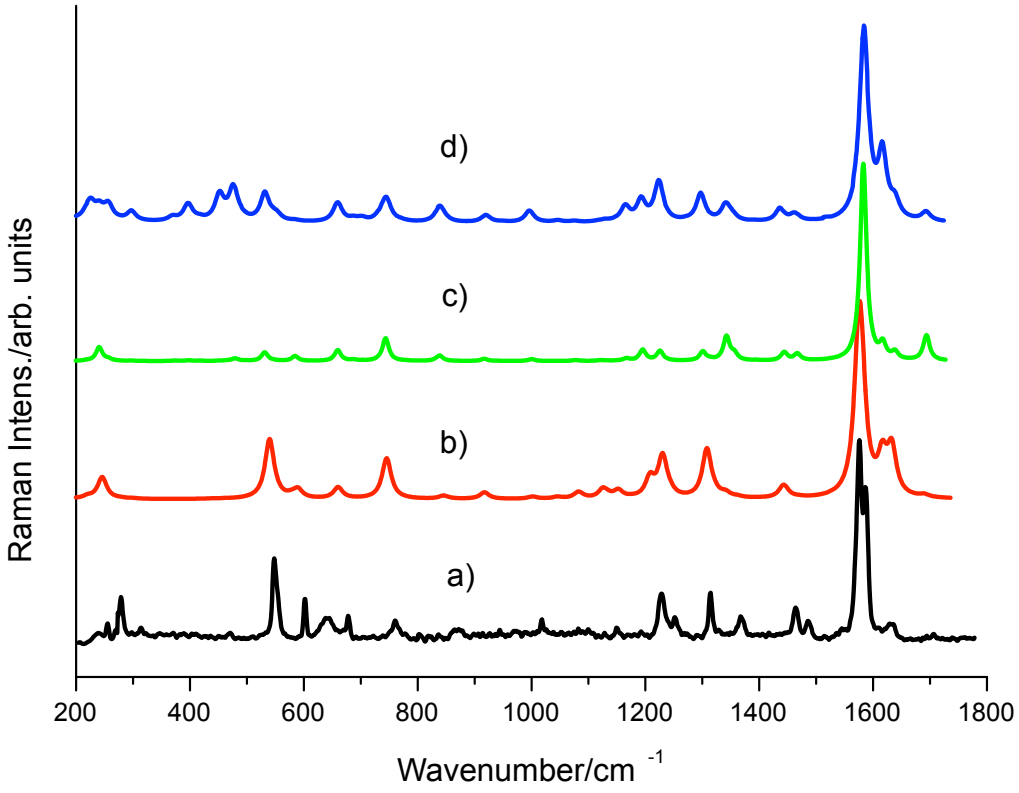

Figure 6: Experimental SERS spectrum of indigo at 785 nm: a); calculated pre-resonance (at 690 nm) Raman spectra of: b) indigo-Ag_2, c) indigo-Ag_{14} edge-on, d) indigo-Ag_{14} surface-on, complexes; spectra are normalized; intensity correction (see Eq. 2) applied

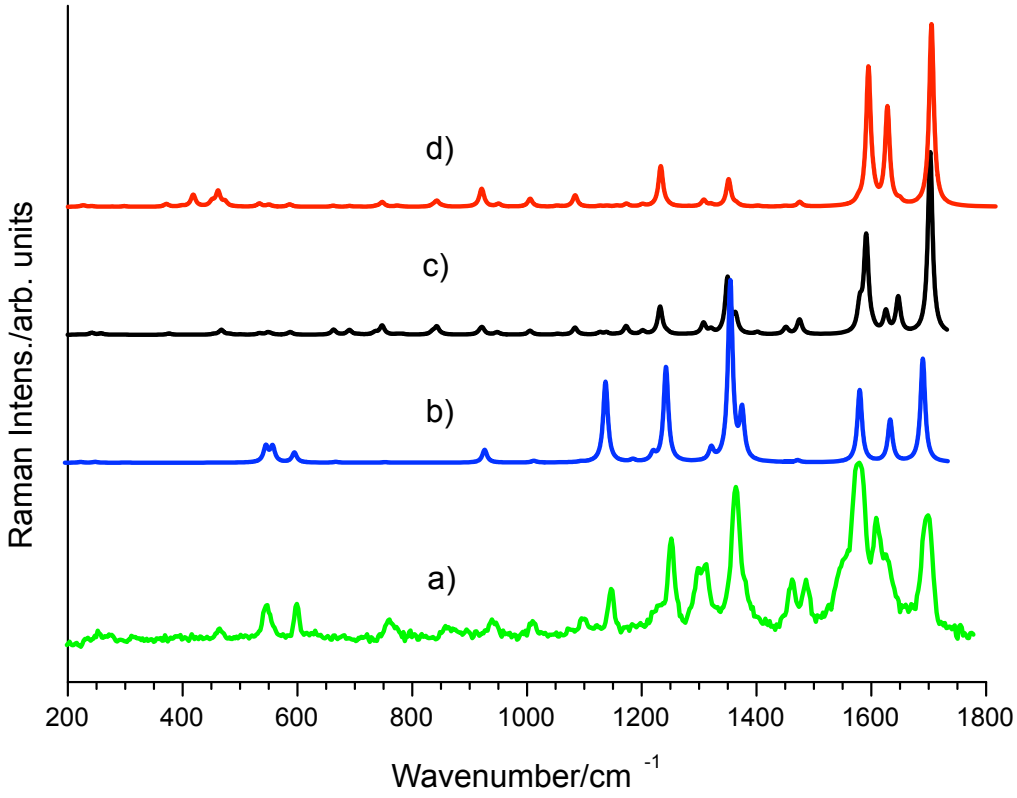

Figure 7: Experimental SERS spectrum of indigo at 514 nm: a); calculated pre-resonance (at 475 nm) Raman spectra of: b) indigo-Ag_2, c) indigo-Ag_{14} edge-on, d) indigo-Ag_{14} surface-on, complexes; spectra are normalized; intensity correction (see Eq. 2) applied

5. Conclusion

The similarity of the experimental Raman and SERS spectra of indigo at 785 nm has been discussed in terms of a very minor reduction of symmetry of the molecule after adsorption on the silver surface and of the absence of effects due to the molecular and plasmonic resonance as well. The proximity of the 514 nm excitation to the molecular absorption and probably, more effective, to the plasmon resonance, enhances instead the SERS intensity such that also new bands become observable. These bands have been identified as IR active bands in the spectrum of the free molecule which become Raman active by the reduction of symmetry from C_{2h} of the free molecule to C_s of the molecule adsorbed on the metal surface. The correlation is from A_g and B_u to A' (in-plane) and from B_g and A_u to A'' (out-of-plane).

The absence of a detectable enhancement of the out-of-plane (A'' under C_s) modes of the molecule in the SERS spectra seems to exclude the possibility that the molecule be adsorbed flat on the surface. If this were the case surface selection rules would have expected a consistent enhancement of the out of plane modes intensity in the SERS spectra. The surface H-T selection rules applied to the edge-on complex predict instead only A' bands to be present with appreciable intensity in the SERS spectra (see Eq. 5 and Ref. [14]). The SERS spectra of indigo obtained with excitation at 514 nm and 785 nm comply with this prediction.

The TD-DFT calculation of the structure, excitation electronic energies and static and pre-resonance vibrational Raman spectra of molecules adsorbed on small silver clusters turned out to be a useful tool for the study of the structural and spectroscopic properties (Raman and SERS) of really adsorbed molecules on silver nanoparticle surfaces [5]. In general, by the DFT simulation only the so-called chemical enhancement effect, which is part of the total spectral enhancement known as SERS, can be modeled. The spectral enhancement for the calculated spectra of the two complexes is much higher in the case of 475 nm excitation (corresponding experimental excitation wavelength 514 nm) than in the case of 690 nm excitation (experimental 785 nm). This corresponds to the presence in the range of excitation of numerous electronic transitions of intra-cluster, charge-transfer and molecular type. In many cases the characterization of the specific transition associated

with an excited state is not feasible as the state is described by a substantial list of orbital transitions with coefficients that are similar in magnitude, without any single dominant component. Natural Transition orbitals (NTOs) has been a helpful way of obtaining a qualitative description of electronic excitations. The ordinary orbital representation of transitions has been transformed into a more compact form in which each excited state is expressed usually as a single pair of orbitals, i.e., HOMO-LUMO, with dominant coefficients.

Lower spectral enhancement is obtained for the calculated Raman spectra of the two complexes at 690 nm (experimental 785 nm). Although the low amplification is justified by the absence in that range of excitation of intra-cluster and intra-molecular electronic excitations, numerous CT transitions occur in the 690 nm spectral range. The intensification of the Raman spectrum of the edge-on complex obtained with the 690 excitation could then originate a resonance type scattering process which relays on CT transitions and which could properly be accounted for by the Albrecht/Lombardi A term. In this case the exclusive presence of totally symmetric bands (A' species) is also justified.

In conclusion, two different geometries of interaction between molecule and metal cluster have been devised, i.e., edge-on and surface-on, whose calculated Raman spectra fairly compare with the experimental ones. The parameters exhibited by the edge-on model, i.e., shifts, appearance of almost exclusively A' (in-plane) species bands in the spectra, intensification, seem better compare with the characteristics of the experimental SERS spectra at 785 and 514 nm and favor this model as the more reliable adsorption geometry of the indigo molecule on the silver nanoparticle surface. Besides, the Herzberg-Teller surface selection rules devised by Lombardi et. al. [14], and applied to the SERS spectra at 785 and 514 nm excitations, as well as the presence in the SERS spectra of IR bands of the free molecule, strongly support the edge-on adsorption geometry. The results of the spectral calculation for the edge-on and the IND-Ag_2 complexes show close similarity, depending on the similar chemical interaction between metal and molecule, where the silver cluster is facing the same type of atomic groups of the molecule, i.e., $C = O$ and NH.

6. Aknowledgements

This work has been supported by the Italian MIUR (grant n. 20100329WPF_007), Laserlab-Europe, H2020 EC-GA 654148 and the Ente Cassa di Risparmio di Firenze (grant n. 2016/13363).

[1] C. Lofrumento, E. Platania, M. Ricci, M. Becucci, E. M. Castellucci, SERS Spectra of Alizarin Anion-Ag_n (n = 2, 4, 14) Systems: TDDFT Calculation and Comparison with Experiment, J. Phys. Chem. C 120 (2016) 12234–12241. doi:10.1021/acs.jpcc.5b12321.

[2] M. Ricci, Elena, C. Lofrumento, E. M. Castellucci, M. Becucci, Resonance Raman Spectra of o-Safranin Dye, Free and Adsorbed on Silver Nanoparticles: Experiment and Density Functional Theory Calculation, J. Phys. Chem. A 120 (2016) 5307–5314. doi:10.1021/acs.jpca.6b01597.

[3] M. Ricci, C. Lofrumento, M. Becucci, E. M. Castellucci, The Raman and SERS Spectra of Indigo and Indigo-Ag_2 Complex: DFT Calculation and Comparison with Experiment, Spectrochim. Acta part A 188 (2018) 141–148. doi:10.1016/j.saa.2017.06.036.

[4] C. Lofrumento, E. Platania, M. Ricci, C. Mulana, M. Becucci, E. M. Castellucci, The sers spectra of alizarin and its ionized species: the contribution of the molecular resonance to the spectral enhancement, Journal of Molecular Structure 1090 (2015) 98–106. doi:10.1016/j.molstruc.2015.01.037.

[5] L. Jensen, L. L. Zhao, G. C. Schatz, Size-Dependence of the Enhanced Raman Scattering of Pyridine Adsorbed on Ag_n (n= 2-8, 20) Clusters, J. Phys. Chem. 111 (2007) 4756–4764. doi:10.1021/jp067634y.

[6] L. Jensen, C. M. Aikens, G. C. Schatz, Electronic structure methods for studying surface-enhanced raman scattering, Chem. Soc. Rev. 37 (2008) 1061–1073. doi:10.1039/B706023H.

[7] A. Amat, F. Rosi, C. Miliani, A. Sgamellotti, S. Fantacci, Theoretical and Experimental investigation on the Spectroscopic properties of indigo dye, J. Mol. Structure 993 (2011) 43–51. doi:10.1016/j.molstruc.2010.11.046.

[8] H. Ajiki, F. Pozzi, L. Huang, L. Massa, M. Leona, J. R. Lombardi, Raman Spectrum of Monobromoindigo, J. Raman Spectrosc. 43 (2012) 520–525. doi:10.1002/jrs.3066.

[9] T. Karapanayiotis, S. E. J. Villar, R. D. Bowen, H. G. M. Edwards, Raman Spectroscopy and Structural Studies of Indigo and its Four 6,6'-Dihalogeno Analogues, Analyst 129 (2004) 613–618. doi:10.1039/B401798F.

[10] A. Baran, A. Fiedler, H. Schulz, M. Baranska, In situ Raman and Ir Spectroscopic Analysis of Indigo Dye, Anal. Methods 2 (2010) 1372–1376. doi:10.1039/c0ay00311e.

[11] M. S. del Rio, M. Picquart, E. Haro-Poniatowski, E. van Elslande, V. H. Uc, On the Raman Spectrum of Maya Blue, J. Raman Spectrosc. 37 (2006) 1046–1053. doi:10.1002/jrs.1607.

[12] E. Platania, C. Lofrumento, E. Lottini, E. Azzaro, M. Ricci, M. Becucci, Tailored Micro-Extraction Method for Raman/SERS Detection of Indigoids in Ancient Textiles, Anal. Bioanal. Chem. 407 (2015) 6505–6514. doi:10.1007/s00216-015-8816-x.

[13] M. Moskovits, Surface selection rules, J. Chem. Phys. 77 (9) (1982) 4408–4416.

[14] J. R. Lombardi, R. L. Birke, A Unified Approach to Surface-Enhanced Raman Spectroscopy, J. Phys. Chem. C 112 (2008) 5605–5617. doi:10.1021/jp800167v.

[15] L. L. Zhao, L. Jensen, G. C. Schatz, Pyridine-Ag_{20} cluster: a model system for studying surface-enhanced raman scattering, J. Am. Chem. Soc. 128 (2006) 2911–2919. doi:10.1021/ja0556326.

[16] M. J. Frisch, G. W. Trucks, H. B. Schlegel, G. E. Scuseria, M. A. Robb, J. R. Cheeseman, G. Scalmani, V. Barone, B. Mennucci, G. A. Petersson, H. Nakatsuji, M. Cari-

cato, X. Li, H. P. Hratchian, A. F. Izmaylov, J. Bloino, G. Zheng, J. L. Sonnenberg, M. Hada, M. Ehara, K. Toyota, R. Fukuda, J. Hasegawa, M. Ishida, T. Nakajima, Y. Honda, O. Kitao, H. Nakai, T. Vreven, J. A. Montgomery, JR., J. E. Peralta, F. Ogliaro, M. Bearpark, J. J. Heyd, E. Brothers, K. N. Kudin, V. N. Staroverov, R. Kobayashi, J. Normand, K. Raghavachari, A. Rendell, J. C. Burant, S. S. Iyengar, J. Tomasi, M. Cossi, N. Rega, J. M. Millam, M. Klene, J. E. Knox, J. B. Cross, V. Bakken, C. Adamo, J. Jaramillo, R. Gomperts, R. E. Stratmann, O. Yazyev, A. J. austin, R. Cammi, C. Pomelli, J. W. Ochterski, R. L. Martin, K. Morokuma, V. G. Zakrzewski, G. A. Voth, P. Salvador, J. J. Dannenberg, S. Dapprich, A. D. Daniels, . Farkas, J. B. Foresman, J. V. Ortiz, J. Cioslowski, D. J. Fox, Gaussian09 Revasion A.01, Gaussian Inc., Wallingford, CT, USA (2009).

[17] E. Tatsch, B. Schrader, Near-infrared fourier transform raman spectroscopy of indigoids, J. Raman Spectrosc. 26 (6) (1995) 467–473. doi:10.1002/jrs.1250260611.

[18] G. Placzek, The Rayleigh and Raman Scattering, translated from: Handbuch der Radiologie, Ed. Erich Marx, Akademische Verlagsgesellschaft VI, 2, 209-374, Leipzig, 1934.

[19] J. R. Lombardi, R. L. Birke, A Unified Approach to Surface-Enhanced Raman Spectroscopy, J. Phys. Chem. C 112 (2008) 5605–5617. doi:10.1021/jp800167v.

[20] A. C. Albrecht, On the theory of Raman Intensities, J. Chem. Phys. 34 (1961) 1476–1484.

[21] R. L. Martin, Natural Transition Orbitals, J. Chem. Phys. 118 (2003) 4775–4777. doi:10.1063/1.1558471.